Materials Transactions

Thermodynamic Description of the Mg-Mn, Al-Mn and Mg-Al-Mn Systems Using the Modified Quasichemical Model for the Liquid Phases

Mohammad Asgar-Khan* and Mamoun Medraj

Department of Mechanical Engineering, Concordia University, Montreal, Quebec, H3G 2B9, Canada

A self-consistent thermodynamic model of the Mg-Mn, Al-Mn and Mg-Al-Mn systems has been developed. The major difference between this work and the already existing assessments of these systems is the application of the modified quasichemical model for the liquid phase in each system while most of the existing descriptions use the random mixing model. In the absence of key data for the Mg-Mn system, the calculated thermodynamic properties from the model have been found comparable to other similar systems and the estimated critical temperature of the Mg-Mn liquid miscibility gap using the available empirical equation has been found to be in acceptable agreement with the calculated value. A comparison between the current work and the most recent work on the Al-Mn system that uses the same model for the liquid phase reveals that better agreement with the experimental data with less number of model parameters has been achieved in the current work. Kohler symmetric extrapolation model with only one ternary interaction parameter has been used to calculate the ternary Mg-Al-Mn system. The thermodynamic description of the Mg-Al-Mn system has been verified by extensive comparison with the available experimental data from numerous independent experiments. The model can satisfactorily reproduce all the invariant points and the key phase diagram and thermodynamic features of the ternary as well as the constituent binary systems. [doi:10.2320/matertrans.MRA2008484]

(Received December 24, 2008; Accepted February 20, 2009; Published April 15, 2009)

Keywords: *thermodynamic modeling, quasichemical model, magnesium-aluminum-manganese, ternary phase diagram, magnesium alloys, aluminum alloys*

1. Introduction

Aluminum and manganese are two of the most important alloying elements for the Mg-based alloys. Having a reliable thermodynamic description of the Mg-Al-Mn system is thus an essential requirement for understanding and predicting the system behavior in many practical applications such as design of experiments, solidification and heat treatment processes etc. The present study deals with the thermodynamic modeling, within the CALPHAD framework, of the Mg-Al-Mn systems which is one of the most important parts of the desired multi-component Mg alloy database. In the current work, Modified Quasichemical Model (MQC), as proposed by Pelton *et al.*,[1] has been used to describe the liquid solution phases in each system. The Mg-Mn and the Al-Mn binaries have been evaluated and modeled in the present study and the remaining Mg-Al system has been taken from Ref. 2). The current work offers a self consistent thermodynamic model for the Mg-Al-Mn systems which can be combined with other existing databases.[2–7]

2. Experimental Data and Earlier Assessments

The available experimental information on the phase equilibria and thermodynamic properties of the Al-Mn, Mg-Mn and Mg-Al-Mn systems and the earlier assessments carried out by different researchers are discussed in the following sections.

2.1 Al-Mn system

Al-Mn phase diagram is characterized by a large number of stable phases in the system. McAlister and Murray[8] critically reviewed the experimental information on the Al-Mn system that were available prior to 1987 and provided their assessment on the system. Jansson[9] made some simplifications of the phase relationships of the Al-Mn system as compared to the assessed phase diagram of[8] and presented a thermodynamic description of the system throughout the entire composition region for the first time. However, the HCP phase at the middle of the Al-Mn phase diagram was not correctly described by Jansson's model because of the probable inaccuracy of the experimental data available at that time. Liu *et al.*[10] used more accurate fixed temperature technique (diffusion couple) for measuring such steep phase boundary features of the intermediate HCP phase and reported the phase equilibria data which were significantly different from the earlier available data. Based on their own experimental results, Liu *et al.*[11] re-modeled the Al-Mn system. Müller *et al.*[12] used Differential Thermal Analysis (DTA), Optical Microscopy (OM), Scanning Electron Microscope (SEM) and X-ray Diffraction (XRD) to measure the equilibrium liquidus and solidus curve for the HCP phase. Liu *et al.*[11] ignored the data of Ref. 12) while Okamoto[13] included it in their assessment of the Al-Mn system. Also, Liu *et al.*[11] did not consider the Mn solubility data of Refs. 14–17) as stated by Ref. 18). Du *et al.*[18] re-modeled the Al-Mn system based on their own DTA, XRD, SEM and Energy Dispersive Spectrometry (EDS) results in the Al-rich side. They[18] included the high temperature modification of the $Al_{11}Mn_4$ phase and the λ-Al_4Mn phase whose existence was questioned by Okamoto[13] due to its close proximity to μ-Al_4Mn. However, the thermodynamic modeling of the Al-Mn system[9,11,18] were using the random solution model for the liquid phase. Recently, Shukla and Pelton[19] published a thermodynamic description of the Al-Mn and Mg-Al-Mn systems using the MQC model for the liquid phases. The calculated results of their[19] work have been compared with the current calculation in section 4.1.

The stable phases in the Al-Mn system, the existence of which are established by the experimental results and

*Graduate Student, Concordia University

Table 1 Stable phases in the Al-Mn system and model used in the current work.

Stable phases	Description	As modeled (current work)	Model used*
(Al)	Terminal solid solution	Gamma (FCC)	SSM
$Al_{12}Mn$	Stoichiometric	$Al_{12}Mn$	ST
Al_6Mn	Stoichiometric	Al_6Mn	ST
λ-Al_4Mn	Stoichiometric	—	Ignored
μ-Al_4Mn	Compound with very limited solubility range	Al_4Mn	ST
$Al_{11}Mn_4$ (HT)	Compound with very limited solubility at high temperature	$Al_{11}Mn_4$	ST
$Al_{11}Mn_4$ (LT)	Stoichiometric phase at low temperature	$Al_{11}Mn_4$	ST
γ_1	Compound with considerable solubility range	Al_8Mn_5	CEF (Three Sublattice)
γ_2	Compound with considerable solubility range	Al_8Mn_5	CEF (Three Sublattice)
γ	Intermediate solid solution	Delta (BCC)	SSM
ε	Intermediate solid solution	Epsilon (HCP)	SSM
δ_{Mn}	Terminal solid solution	Delta (BCC)	SSM
γ_{Mn}	Terminal solid solution	Gamma (FCC)	SSM
β_{Mn}	Terminal solid solution	Beta (CUB)	SSM
α_{Mn}	Terminal solid solution	Alpha (CBCC)	SSM

*CEF - Compound Energy Formalism, SSM - Substitutional Solution Model, ST - Stoichiometric Compound

thermodynamic assessments of the previous researchers have been listed in Table 1. The terminology and the models used in the current work in describing the Gibbs energy of all these phases are also shown in the table.

A number of experimental thermodynamic information is also available for the Al-Mn system. Esin[20] measured calorimetrically the enthalpy of mixing of liquid Al-Mn at 1353°C. Batalin[21] measured the activity of Al in liquid Al-Mn alloy at 1297°C by EMF measurement and Chastel *et al.*[22] measured the same at 1247°C using Knudsen cell. Kubaschewski and Heymer[23] and Meschel and Kleppa[24] measured the enthalpy of formation of some of the solid Al-Mn alloys using, respectively, reaction calorimetry and direct synthesis calorimetry. Kematick and Myers[25] investigated the Al-Mn system using Knudsen cell-mass spectrometry and measured the activities of Al and Mn in some of the solid alloys at 902°C. All these data have been taken into consideration in the present assessment and compared with the current calculation.

2.2 Mg-Mn system

Mg-Mn system is characterized by a wide miscibility gap in the liquid. Very limited experimental data are available for the Mg-Mn system and the available data are inconsistent among one-another. Most of the available data are on the Mg-rich side describing the limited solid solubility of Mn in Mg. Hashemi and Clark[26] critically assessed the experimental data available on this system and summarized the reliable data. Further discussion on these experimental results are not given here as their[26] assessment was found reliable. No evidence on the solid solubility of Mg in Mn or experimental information could be found in the literature. Gröbner *et al.*[27] examined the phase diagram at high temperature and reported a monotectic reaction temperature in the Mg-Mn system using the DTA technique. In addition to this experiment, they[27] modeled the system with the random solution model for the liquid phase. Their model calculates the consolute temperature of the liquid miscibility gap of the Mg-Mn system at 3202°C.[28] Antion[29] questioned the existence of very high consolute temperatures of the binary miscibility gap based on the experimental observation of the consolute temperature of the ternary Mg-Mn-Y system. Kang *et al.*[28] optimized the Mg-Mn system using the MQC model for the liquid phase with simultaneous consideration of the experimental data in the Mg-Mn-Y ternary system. Their optimization results in a consolute temperature of Mg-Mn liquid miscibility gap to be 1902°C which is much lower than that of the earlier model of Gröbner *et al.*[27] In the absence of key experimental information in the lower order system, especially, when contradicting results are found by different independent assessments like in Refs. 27, 28), it is interesting to compare the thermodynamic properties with similar binary systems. Although this is not as accurate as comparing with experimental data, this procedure will provide guidelines for the trends and order of magnitude of the needed thermodynamic properties.

2.3 Mg-Al-Mn system

Numerous researchers[18,19,30–47] investigated the phase equilibria of the ternary Mg-Al-Mn system. All the experimental data are available near the Mg-Al edge of the ternary system. One ternary stoichiometric phase has been reported by Ref. 46) and no experimental information on the Mn rich side of the ternary was found in the literature. Ohno and

Schmid-Fetzer[30] critically reviewed the earlier experimental data and assessments and presented the thermodynamic modeling of the system with the parameters which were primarily optimized on the basis of the Mn solubility data of Beerwald,[47] Nelson[32] and Thorvaldsen and Aliravci.[36] On the other hand, Du *et al.*[18] reassessed the Al-Mn binary system based on their own experimental data at the Al-rich side and presented the thermodynamic model for the ternary Mg-Al-Mn system for the entire composition range. They[18] reviewed the previous experimetnal investigations on the Al-rich part of the ternary system and compared the data of Fahrenhorst and Hoffmann,[39] Wakeman and Raynor[42] and Ohnishi *et al.*[43,44] with their calculated results because of the consistency of these data. The current calculations are also compared with these data[39,42–44] for the Al-rich part of the Mg-Al-Mn system. Since the reviews of Ohno and Schmid-Fetzer[30] and Du *et al.*[18] of the previous experimental investigations on the ternary Mg-Al-Mn system seem reasonable, these are not discussed further to avoid duplication. However, it should be noted that these two previous modeling on the ternary Mg-Al-Mn system[18,30] were done with the random solution model for the liquid phase.

3. Gibbs Energy Models

Gibbs energy of each of the stable phases of the ternary and constituent binary systems has been described by the most representative thermodynamic models in the current work. The modeling and the optimization are carried out with the aid of the thermo-chemical software FactSage.[48] The lattice stabilities of the pure elements Mg, Al and Mn have been taken from Ref. 49). The terminal solid solutions as well as the intermediate delta (BCC) and epsilon (HCP) phases in the Al-Mn system are modeled with the Substitutional Solution Model (SSM) taking into account the crystal structure data[13,50–52] of the phases. The intermediate solid solution Al_8Mn_5 in the Al-Mn system are modeled using the Compound Energy Formalism (CEF) with three sublattices as proposed by Jansson.[9] The stable line compounds in the Al-Mn and Mg-Al-Mn systems as well as the Mn CBCC and CUB phases in the Mg-Mn system have been modeled as stoichiometric phases in this work.

3.1 Choice of the MQC model for the liquid phase

The choice of the appropriate model for a phase is one of the key steps in modeling a system in the CALPHAD approach. The liquid solution phases in the Mg-Mn, Al-Mn and Mg-Al-Mn systems have been modeled with the MQC model instead of the Bragg-Williams (BW) (i.e. random-mixing) model in the current work. The detailed description of the MQC model is given in Ref. 1) and the key aspects of the model are briefly discussed below.

The governing equation for this model is:

$$\Delta g_{AB} = \Delta g^{o}_{AB} + \sum_{i\geq 1} g^{i0}_{AB} X^{i}_{AA} + \sum_{j\geq 1} g^{0j}_{AB} X^{j}_{BB}$$

where, Δg_{AB} is the change in the Gibbs energy for the formation of 2 moles of A-B pair from one mole of (A-A) and one mole of (B-B) pair according to the pair exchange reaction (A-A) + (B-B) = 2(A-B). A and B denote the atoms of the elements which are distributed over a quasi-lattice. The X_{AA} is the pair fraction defined as the ratio of the number of moles of (A-A) pairs to the total number of moles of (A-A), (B-B) and (A-B) pairs. The Δg^{o}_{AB}, g^{i0}_{AB} and g^{0j}_{AB} are the parameters of the model to be optimized and may be temperature dependent. It is to be noted here that unlike the BW model, the configurational entropy is approximated in MQC model by randomly distributing the pairs over the 'pair sites' over the quasilattice. The coordination numbers Z_A and Z_B of atoms A and B are permitted to vary according to the following equations:

$$\frac{1}{Z_A} = \frac{1}{Z^A_{AA}}\left(\frac{2n_{AA}}{2n_{AA}+n_{AB}}\right) + \frac{1}{Z^A_{AB}}\left(\frac{n_{AB}}{2n_{AA}+n_{AB}}\right)$$

$$\frac{1}{Z_B} = \frac{1}{Z^B_{BB}}\left(\frac{2n_{BB}}{2n_{BB}+n_{AB}}\right) + \frac{1}{Z^B_{BA}}\left(\frac{n_{AB}}{2n_{BB}+n_{AB}}\right)$$

where, all Z^i_{ii} are coordination number of atom i when surrounded by the same type of atoms and Z^i_{ij} are the coordination number of atom i when the surrounding atoms are dissimilar.

The major advantage of the proposed modified model is that it expands the Gibbs energy function of the solution phase in terms of pair fractions instead of equivalent fraction which offers greater flexibility in optimizing the parameters for the systems, especially for systems which show a large degree of short range ordering in the liquid phase.[1] It is physically more realistic in a sense that it considers the preferential formation of nearest neighbor A-B pairs for the short range ordering. Nevertheless, it reduces to the ideal solution model for the random mixing approximation.[1] Thus even for a specific binary or a ternary system where the presence of short range ordering in the liquid is not evident, the choice of the modified quasichemical model is still justified. Further, the model allows choosing freely the composition of the maximum short range ordering in the liquid in the binary system by choosing a suitable composition dependent hypothetical coordination number. Finally, the choice of the modified quasichemical model for the liquid phase leads to the required consistency with the other existing databases,[2–7] developed with the same model for Mg alloys. Successful application of this model for the optimization of numerous binary and higher order systems provides the basis for choosing the model for optimizing the current ternary and the binary subsystems.

4. Results and Discussions

The process of the current thermodynamic modeling results in a set of model parameters that describe the Gibbs energy function of all the phases in the Mg-Mn, Al-Mn and Mg-Al-Mn systems. The optimized parameters for the Al-Mn, Mg-Mn and Mg-Al-Mn systems are listed in Tables 2, 3 and 4, respectively. The values of the composition dependent coordination numbers used in the MQC model for all the atoms in different phases have been chosen to be 6 except for the coordination number of the Mg-Mn pairs, designated as Z^{Mg}_{MgMn}, which has been chosen to be 4. This choice of the hypothetical coordination numbers ensures the required consistency with the other existing databases[2–7] on one hand

Table 2 The optimized parameters of the stable phases in the Al-Mn system.

Phase	Model*	Parameters	J·mol^{-1}·atom^{-1}	J·mol^{-1}·atom^{-1}·K^{-1}
Liquid	MQC	Δg^{o}_{AlMn}	−18 367.76	6.527
		g^{10}_{AlMn}	−7 154.64	2.761
$Al_{12}Mn$	ST	$\Delta G_{Al_{12}Mn}$	−8 400.38	2.597
Al_6Mn	ST	ΔG_{Al_6Mn}	−15 124.29	4.227
Al_4Mn	ST	ΔG_{Al_4Mn}	−20 590.00	5.621
$Al_{11}Mn_4$	ST	$\Delta G_{Al_{11}Mn_4}$	−22 246.67	4.664
Alpha (CBCC)	SSM	^{o}L	−79 106.89	40.627
		^{1}L	−14 476.64	0.0
Gamma (FCC)	SSM	^{o}L	−44 275.09	3.556
Epsilon (HCP)	SSM	^{o}L	−1 01 708.86	36.07
		^{1}L	−8 280.14	5.146
		^{2}L	1 32 758.32	−83.178
Delta (BCC)	SSM	^{o}L	−1 22 800.40	51.04
		^{1}L	67 362.40	−41.171
Al_8Mn_5	CEF, three sublattices	$^{o}G_{Al:Mn:Al}$	−16 418.98	5.568
		$^{o}G_{Al:Mn:Mn}$	−26 001.95	5.944
		^{o}L	−12 133.60	3.981
Beta (CUB)	SSM	^{o}L	−1 10 959.68	41.873
		^{1}L	−21 756.80	25.90

*CEF - Compound Energy Formalism, SSM - Substitutional Solution Model, ST - Stoichiometric compound

Table 3 The optimized parameters of the stable binary phases in Mg-Mn system.

Phase	Model*	Parameters	J·mol^{-1}·atom^{-1}	J·mol^{-1}·atom^{-1}·K^{-1}
Liquid	MQC	Δg^{o}_{MgMn}	22 973.44	0.808
		g^{10}_{MgMn}	−11 995.18	0.0
Mg (HCP)	SSM	^{o}L	46 643.23	−8.828
		^{1}L	−3 322.10	0.0
Gamma (FCC)	SSM	^{o}L	83 680.00	0.0
Delta (BCC)	SSM	^{o}L	83 680.00	0.0

*SSM - Substitutional Solution Model

Table 4 The optimized parameters for the stable ternary phases in Mg-Al-Mn system.

Phase	Model*	Parameters	J·mol^{-1}·atom^{-1}	J·mol^{-1}·atom^{-1}·K^{-1}
Liquid	MQC	$\Delta g^{o}_{Al,Mn:Mg}$	15 480.80	0.0
$Mg_3Al_{18}Mn_2$ (T)	ST	$\Delta G_{Mg_3Al_{18}Mn_2}$	−8 695.65	0.006

*ST - Stoichiometric compound

while giving the best description of the systems. The notion for the best description of a system is associated with the capability of the model parameters to consistently reproduce the reliable experimental phase equilibria and thermodynamic data. With the optimized parameters listed above, all the calculated phase equilibria and thermodynamic properties in relation to the accepted experimental results for the Al-Mn, Mg-Mn and Mg-Al-Mn systems have been discussed in detail in the following sections.

4.1 Al-Mn system

The calculated Al-Mn phase diagram with their stable equilibrium phases is shown in Fig. 1. The corresponding calculated invariant reactions and the compositions of the respective phases are given in Table 5.

The calculated Al-Mn phase diagram has an overall good agreement with the accepted experimental results as shown in Figs. 2 through 4. The calculated solid solubility of Mn in Al has been compared with the solubility measurements of Refs. 14–17, 39, 53–56) and the calculation of the most recent work of Shukla and Pelton[19] on this system as shown in Fig. 2. The current calculation almost reproduces the EPMA results of Minamino *et al.*[15] while showing a good agreement with the mutually consistent data. The calculation of Ref. 19) is also acceptable considering the uncertainty of the experimental results although the agreement with a particular set of data is not evident.

The calculated Al-rich portion (< 45 at%, Mn) is shown in Fig. 3. Only the thermal analyses heating data rather than the cooling data of Refs. 18, 55, 57–60) have been compared here in order to avoid the inconsistencies that might result from possible undercooling effect. The reliable data in this region are well reproduced in the calculation.

It is to be noted here that the near stoichiometric phase μ-Al_4Mn, of which, Okamoto[13] questioned the existence because of its proximity to the other stoichiometric λ-Al_4Mn phase, has been ignored in the current work. Also, the other stable phase which shows a narrow homogeneity range and often termed as the high temperature modification of the $Al_{11}Mn_4$, has been modeled as stoichiometric compound for the sake of simplicity. However, this simplification does not lead to a significant error in the higher order systems as discussed by Jansson.[9] Also, the possible existence of order-disorder transition in the intermediate delta (BCC) phase in the middle of the phase diagram as stated by Liu *et al.*[11] was not modeled in the current work due to lack of experimental evidence.

In Fig. 4, a portion of the calculated phase diagram is compared with the accepted experimental results of Refs. 10, 12, 52, 58–60) and the calculation of Ref. 19).

The current calculation shows a better agreement with the experimental data compared with the calculation of Ref. 19). Also, the current calculation is consistent with the observation of Okamoto[13] who suggested a smooth continuous liquidus curve between the terminal delta (BCC) and intermediate delta (BCC) solid solution phase throughout the epsilon (HCP) phase as mentioned in Ref. 11). The other available calculations[9,11] are also consistent with this observation while the calculated liquidus lines of Ref. 19) did not maintain this condition.

Figure 5 shows that the enthalpy of mixing of the Al-Mn liquid measured by Esin *et al.*[20] showing a large negative value with a minimum around 45 at% Mn has been reproduced satisfactorily in the current calculation.

The activities of the components in the Al-Mn melt measured by Batalin *et al.*[21] and Chastel *et al.*[22] have been compared with the current calculation as well as the

Table 5 Calculated invariant points in the Al-Mn system compared with the experimental data.

Reaction	Type	Temp., T/°C	Composition (at% Mn)			Reference
FCC + Al_6Mn ⇔ $Al_{12}Mn$	Peritectoid	511	0.2	14.3	7.7	This work
		504–521	—	—	—	71)
L ⇔ Gamma (FCC) + Al_6Mn	Eutectic	658	1.0	0.6	14.3	This work
		658	0.99	—	—	58)
L + Al_4Mn ⇔ Al_6Mn	Peritectic	705	2.4	20.0	14.3	This work
		705	—	19.00	—	57)
L + $Al_{11}Mn_4$ ⇔ Al_4Mn	Peritectic	923	14.4	26.7	20.0	This work
		923	15.00	24.20	21.00	57)
L + Al_8Mn_5 ⇔ $Al_{11}Mn_4$	Peritectic	1001	22.6	31.5	26.7	This work
		1002	22.30	30.00	28.00	57)
L + Delta (BCC) ⇔ Epsilon (HCP)	Peritectic	1271	65.5	68.7	67.9	This work
		1260	—	—	—	57)
		1280	—	—	—	10)
		1256	—	—	—	12)
HCP ⇔ Delta (BCC) + Beta (CUB)	Eutectoid	858	56.7	53.2	58.3	This work
		870	—	—	—	57)
		870	55.00	50.05	60.00	52)
		870	58.00	53.50	60.60	10)
		857	—	—	—	12)
L + Delta (BCC) ⇔ Al_8Mn_5	Peritectic	1047	27.5	36.4	36.1	This work
		1048	28.30	34.50	33.60	57)
L + Epsilon (HCP) ⇔ Delta (BCC)	Peritectic	1177	44.8	53.4	51.8	This work
		1160	—	—	—	58)
		1190	—	—	—	12)
Delta (BCC) ⇔ Al_8Mn_5 + Beta (CUB)	Eutectoid	816	52.3	49.8	58.4	This work
		840	49.50	47.00	59.50	57)
		817	—	—	—	12)
Delta (BCC) + Gamma (FCC) ⇔ Beta (CUB)	Peritectoid	1068	89.8	92.5	91.0	This work
			—	—	—	—
Delta (BCC) ⇔ Epsilon (HCP) + Beta (CUB)	Eutectoid	1046	71.4	72.1	76.0	This work
		1040	74.50	71.50	75.50	10)
		903	—	—	—	12)
L ⇔ Delta (BCC)	Congruent	1314	82.8	82.8		This work
			—	—	—	—
Beta (CUB) ⇔ Gamma (FCC)	Congruent	1061	95.7	95.7		This work
			—	—	—	—

calculation of[19] in Fig. 6. The current calculation is consistent with both the experimental data while favoring the more recent data of Chastel *et al.*[22] who used Knudsen effusion cell for their measurements. On the other hand, the calculation of Ref. 19) is not consistent with these data as can be seen in Fig. 6.

In Fig. 7, the experimental enthalpy of formation of some of the solid Al-Mn alloys and the calculated results of Ref. 19) have been compared with the current calculation. The current calculation reproduces the experimental data within the experimental error limits for all the composition of Al-Mn alloy except near the middle composition of the phase diagram. At 50 at% Mn, the current calculation predicts lower enthalpy of formation than the value measured by Kubaschewski and Heymer.[23] It should also be noted that Ref. 23) reported two different values of formation enthalpy for the same composition at 50 at% Mn which may be an indication of significant uncertainty associated with the data at this composition. Nevertheless, the current results are generally closer to the experimental values than those of Ref. 19).

In Fig. 8, the calculated log activity versus composition has been compared with the measured values of Kematick and Myers.[25] They[25] linked the data points of the Mn activities and found that their measurement of the activity of Mn is consistent with the assessed Al-Mn phase diagram of

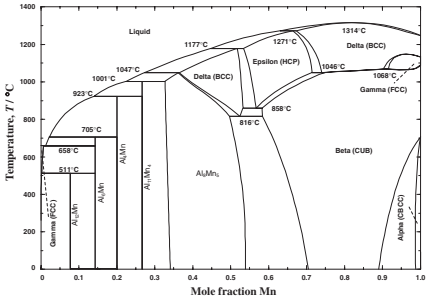

Fig. 1 Calculated Al-Mn phase diagram.

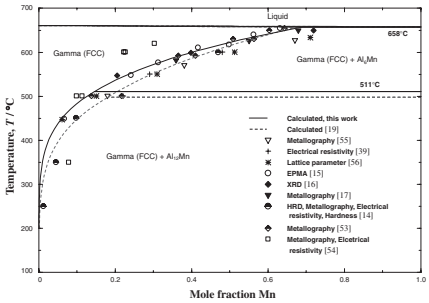

Fig. 2 Calculated solubility of Mn in Al compared with the data measured by Refs. 14–17, 39, 53–56) and the calculation of Ref. 19).

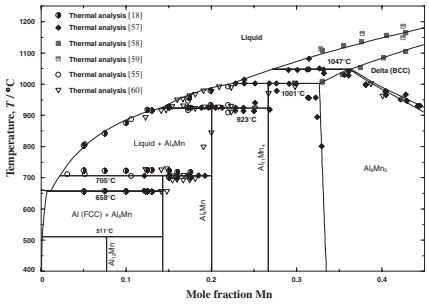

Fig. 3 Calculated Al-rich part of the Al-Mn phase diagram with selected experimental results of Refs. 18, 55, 57–60).

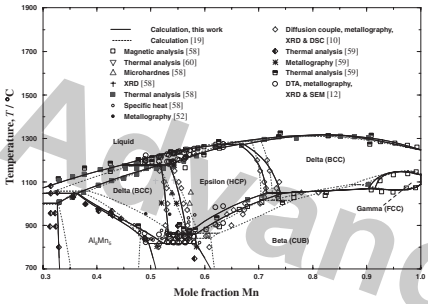

Fig. 4 Calculated Mn-rich portion of the Al-Mn phase diagram compared with the selected experimental results of Refs. 10, 12, 52, 58–60) and the calculation of Ref. 19).

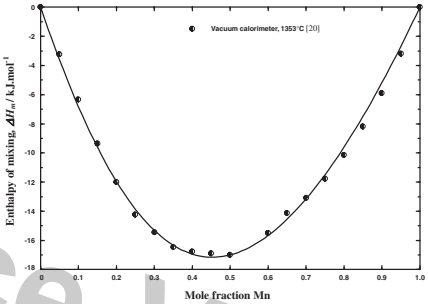

Fig. 5 Calculated enthalpy of mixing of liquid Al-Mn alloy at 1353°C compared with the measured values from Ref. 20).

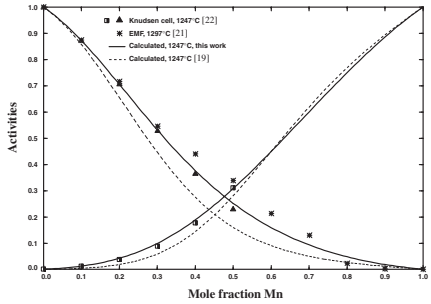

Fig. 6 Calculated activities of Al and Mn in the liquid Al-Mn alloys compared with the measured values from Refs. 21, 22) and calculation of Ref. 19).

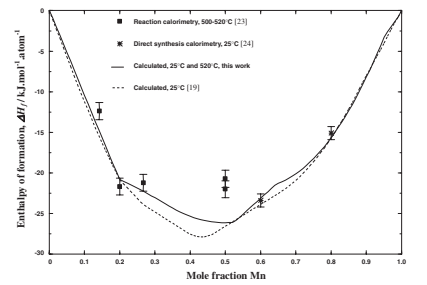

Fig. 7 Calculated enthalpy of formation of some solid Al-Mn alloys compared with the measured values from Refs. 23, 24) and the calculation of Ref. 19).

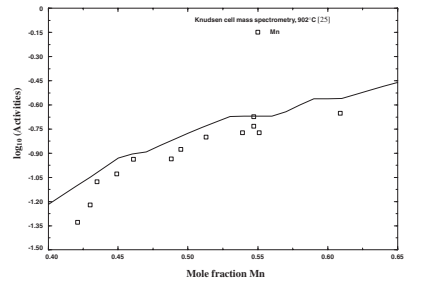

Fig. 8 Comparison of the calculated log activity vs composition with the measured values from Ref. 25).

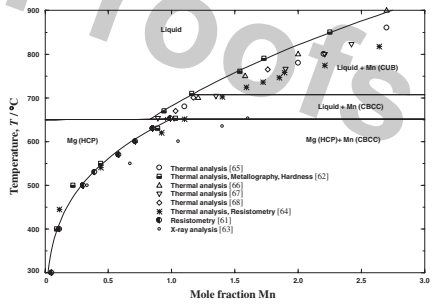

Fig. 9 Comparison of the calculated Mg-rich portion of the Mg-Mn phase diagram with the data from Refs. 61–68).

McAlister and Murray.[8] The current calculation reasonably agrees with the measurements of Mn activities as shown in Fig. 8. In the most recent assessments of the Al-Mn system, Du *et al.*[18] and Shukla and Pelton[19] did not use the data of Ref. 25) claiming it to be inconsistent with the other data of the system.

In Table 6, the number of parameters used for optimizing the Al-Mn system is compared between the current work and the work of Shukla and Pelton[19] who also used the MQC model for the liquid phase. The number of model parameters and coefficients used for the different phases in this work is either less than or equal to that of the work of Ref. 19) as can be seen in Table 6. Further, the agreements with the experimental results are generally better in the current work than in the work of Ref. 19).

4.2 Mg-Mn system

The calculated Mg-rich portion of the Mg-Mn phase diagram has been compared with the experimental data from Refs. 61–68) as shown in Fig. 9. The calculated solubility of Mn in Mg favors the data of Drits *et al.*,[61] Grogan *et al.*[64] and Petrov *et al.*[62] which are self-consistent and deviates from the data of Schmid and Siebel[63] who measured higher Mn content in the solution. Similarly, the liquidus data of Petrov *et al.*[62] who measured higher liquidus temperature is favored in the calculation as shown in Fig. 9. This is because the higher liquidus temperatures were expected considering the sources of error in the dip sampling technique which was used to measure the liquidus curve in the Mg-Mn system. In Fig. 10, the calculated Mg-Mn phase diagram has been compared with the experimental phase diagram data of

Table 6 Comparison of the number of model parameters used for optimizing the Al-Mn system between this work and the work of Ref. 19).

Phase	Model* used	No. of parameters	No. of coefficients	Reference
Liquid	MQC	2	4	This work
		3	6	19)
Alpha (CBCC)	SSM	2	3	This work
		2	3	19)
Beta (CUB)	SSM	2	4	This work
		2	4	19)
Gamma (FCC)	SSM	1	2	This work
		2	4	19)
Delta (BCC)	SSM	2	4	This work
		2	4	19)
Epsilon (HCP)	SSM	3	6	This work
		3	6	19)
Al_8Mn_5	CEF, three sublattices	1	2	This work
		2	4	19)

*CEF - Compound Energy Formalism, SSM - Substitutional Solution Model

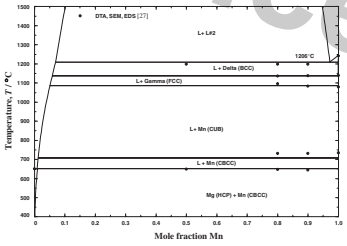

Fig. 10 Comparison of the calculated Mg-Mn phase diagram with the experimentally measured values from Ref. 27).

Ref. 27) who used DTA, SEM and EDS. They[27] measured the binary monotectic temperature whose lower limit was reported to be around 1200°C. The possible underestimation of temperature due to the reaction of the crucible material with the liquid Mn was reported to be the reason for depicting the measured monotectic temperature as the lower limit. The current model calculates the monotectic reaction temperature at 1206°C which is in agreement with the observation of Ref. 27).

In Table 7, some of the calculated thermodynamic properties of the liquid phase in similar binary systems which show extended miscibility gap in the liquid have been compared. The values of the thermodynamic quantities are comparable with the values of the similar systems. Further, the calculated critical temperature of the miscibility gap near the equiatomic composition is found to be 3688 K. This value is also comparable with the model of Ref. 27) which calculates it at 3475 K. The percentage deviation of the current value of the critical temperature, from the estimated value using Predel's[69] empirical equation, falls within the range of the percentage deviation of other similar systems as shown in the last column of Table 7. The authors find it more reasonable to evaluate the current model on the basis of such thermodynamic considerations rather than to use one experimental information in a specific higher order system to validate the reliability of the calculation in a lower order system as performed in Ref. 28). No relevant experimental information on any other ternary systems involving Mg-Mn as a constituent system are available, except the result of Antion,[29] to support the conclusion of Ref. 28) that the critical temperature of the Mg-Mn miscibility gap should be far less than that calculated in Ref. 27). The present calculation relies on the comparison of the thermodynamic quantities with other similar systems which gives a reasonable basis for the reliability of the current model in the absence of relevant experimental information on the Mg-Mn system.

4.3 Mg-Al-Mn system

A series of calculations has been performed for the ternary Mg-Al-Mn system with the constructed database and the outcome has been compared with the experimental results in Figs. 11 through 20. In Fig. 11, the liquidus projection for the entire composition range of the Mg-Al-Mn system has been calculated. The Mg-rich part of the liquidus projection has been zoomed and shown in Fig. 12 with comparison to the available experimental data.

The liquidus projection in the Mg-rich corner of the Mg-Al-Mn system in Fig. 12 shows a reasonable consistency with the experimental data of Simensen *et al.*[34,35] and Thorvaldsen and Aliravci.[36] The calculated invariant reac-

Table 7 Comparison of thermodynamic properties of liquid binary alloys at equiatomic composition exhibiting extended miscibility gap in liquid.[70]

Alloys	Temp., T/(K)	G_M^{xs}/RT[70]	H_M/RT[70]	S_M^{xs}/R[70]	Critical temp., T_{Cr}/K (Estimated) $T_{Cr}^{**} = 2H_m/(R + 2S_M^{xs})$, p	T_{Cr}/K Assessed, q	% deviation $\frac{\lvert p-q\rvert}{q} * 100$
Al-In	1150	0.540	0.490	−0.050	1251	1112	12.5
Al-Pb	1700	0.527	0.847	0.320	1755	1700	3.2
Bi-Zn	880	0.360	0.600	0.240	713	864	17.5
Cd-Ga	695	0.485	0.484	−0.001	337	560	39.8
Mg-Mn*	3723*	0.427*	0.332*	−0.095*	3056	3688*	17.1

*Calculation using the current model
**Estimated using Predel's[69] empirical equation

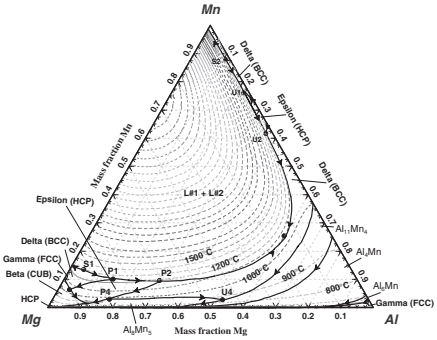

Fig. 11 Calculated liquidus projection with arrows indicating the decreasing temperature.

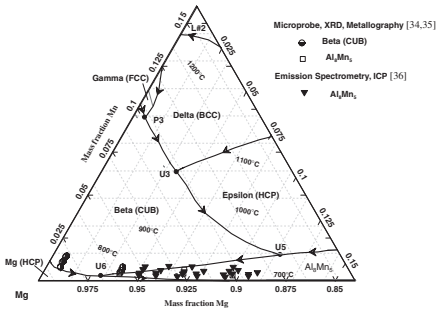

Fig. 12 Liquidus projection in the Mg-rich corner of the Mg-Al-Mn system compared with the data of Refs. 34–36) (Dotted lines are isotherms).

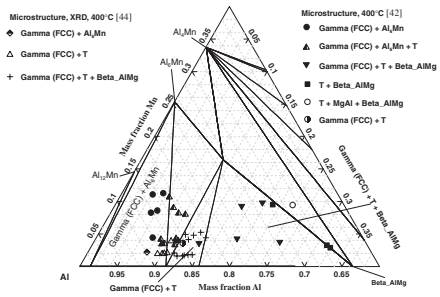

Fig. 13 Calculated isothermal section at 400°C compared with the experimental data of Refs. 42, 44).

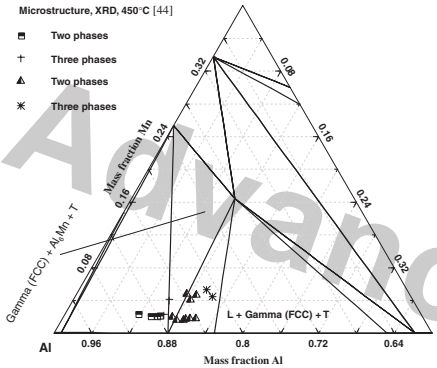

Fig. 14 Calculated isothermal section in the Al-rich corner at 450°C compared with the experimental data of Ref. 44).

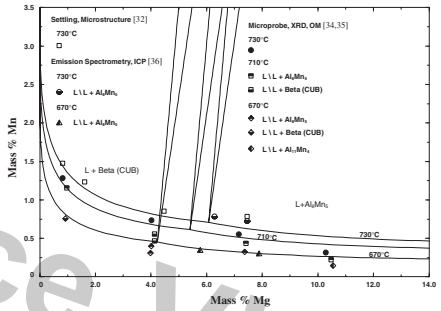

Fig. 15 Calculated isothermal sections in the Mg-rich corner at 670, 710 and 730°C compared with the experimental data of Refs. 32, 34–36).

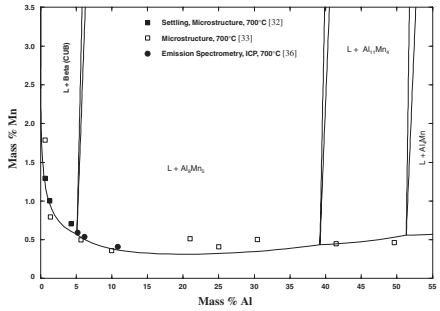

Fig. 16 Calculated isothermal section in the Mg-rich corner at 700°C compared with the experimental data of Refs. 32, 33, 36).

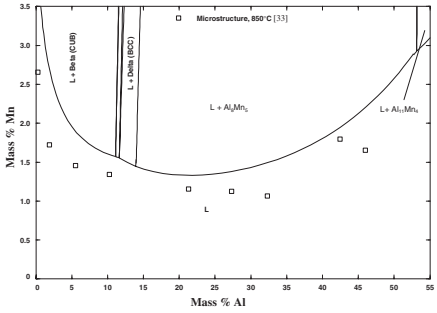

Fig. 17 Calculated isothermal section in the Mg-rich corner at 850°C compared with the experimental data of Ref. 33).

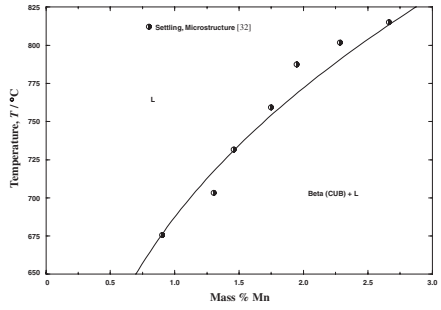

Fig. 18 Calculated vertical section with 0.8 mass% Al compared with the experimental data of Ref. 32).

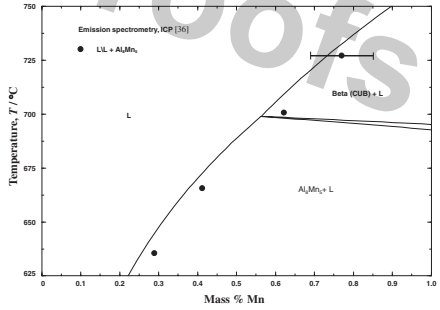

Fig. 19 Calculated vertical section at 5.05 mass% Al compared with the experimental data of Ref. 36).

tions, their type and compositions in the ternary Mg-Al-Mn system have been given in Table 8. Some degenerate invariant points also exist in the proximity of the Mg-Al edge, which have not been shown in the table.

Several isothermal sections, for which reliable experimental information is available, have been calculated for the Mg-Al-Mn ternary system. The calculated isothermal section at 400°C, as shown in Fig. 13, agrees well with the data of Wakeman and Raynor.[42)]

Another isothermal section at 450°C has been compared with the data of Ref. 44) in Fig. 14 which shows reasonable agreement. The deviations of the calculated results from the experimental data, as can be seen in Figs. 13 and 14, are acceptable considering the possible uncertainties in the measurements.

Calculated isothermal sections at 670, 710 and 730°C have been compared with the available experimental data of Refs. 32, 34–36) in Fig. 15. In Figs. 16 and 17, the calculated isothermal sections at 700°C and 850°C, respectively, have been compared with the experimental data of Refs. 32, 33, 36). The experimental liquidus isotherms of Ref. 36) are well reproduced in the calculations as can be seen in Figs. 15 and 16. Although, Nelson,[32)] Mirgalovskaya *et al.*[33)] and Simensen *et al.*[34,35)] did not report the equilibrium phases in some cases, Figs. 15 to 17 show that their liquidus isotherms are also reproduced satisfactorily by the

Table 8 Invariant points in Mg-Al-Mn system according to the current calculation.

Reaction	Temp., T/°C	Type*	Composition (mass%)		
			Mn	Mg	Al
L#1 ⇔ L#2 + Delta (BCC)	1301	S1	13.2	82.8	4.0
L#1 ⇔ L#2 + Delta (BCC)	1301	S2	88.0	1.3	10.6
L#1 + Delta (BCC) ⇔ L#2 + Epsilon (HCP)	1276	U1	75.9	1.6	22.5
L#1 + L#2 + Delta (BCC) ⇔ Epsilon (HCP)	1249	P1	10.7	77.6	11.7
L#1 + Epsilon (HCP) ⇔ L#2 + Delta (BCC)	1216	U2	59.4	2.3	38.3
L#1 + L#2 + Epsilon (HCP) ⇔ Delta (BCC)	1166	P2	9.7	58.0	32.3
L#1 + FCC ⇔ Beta (CUB) + Delta (BCC)	1069	P3	9.4	89.5	1.1
L#1 + Epsilon (HCP) + Delta (BCC) ⇔ Al_8Mn_5	976	P4	3.3	79.2	17.5
L#1 + Delta (BCC) ⇔ Epsilon (HCP) + Beta (CUB)	1029	U3	6.6	90.3	3.1
L#1 + Delta (BCC) ⇔ $Al_{11}Mn_4$ + Al_8Mn_5	846	U4	2.8	44.9	52.3
L#1 + Epsilon (HCP) ⇔ Beta (CUB) + Delta (BCC)	846	U5	1.5	88.7	9.7
L#1 + Beta (CUB) ⇔ Mg (HCP) + Al_8Mn_5	621	U6	0.3	96.7	2.9

*U: Transition type, P: Formation type. S: Saddle point

current model. It should be noted here that the isothermal sections in Figs. 15 to 17 have been drawn on rectangular coordinates instead of triangular in order to enable better viewing and comparison with the experimental data. The isothermal section at 850°C could not be satisfactorily reproduced with the models of Ohno and Schmid-Fetzer[30] and Shukla and Pelton.[19]

The solubility of Mn in the liquid Mg-Al alloys has been compared with the experimental data of Ref. 32) and Ref. 36) in two vertical sections in Figs. 18 and 19, respectively.

Figure 18 shows that, the data of Nelson[32] are in accordance with the current calculation although he did not report the type of the equilibrium phases. However, there is a disagreement in the identification of equilibrium phase between the current calculation and two data points of Thorvaldsen and Aliravci[36] as shown in Fig. 19. These two data points were reported to be in the Al_8Mn_5 phase region by Thorvaldsen and Aliravci[36] who used Emission Spectrometry and Inductively Coupled Plasma (ICP) technique with 0.01 mass% repeatability for manganese and 0.1–0.2 mass% for aluminum, while this calculation detects this as Beta (CUB) region. They[36] proposed a solubility model fitting these chemical analysis data. However, their solubility model did not reproduce the data in the low Al concentrations ($\approx$ 5 mass%) region specially those resulted from high holding temperature (>700°C) experiments. The deviations of compositions in this region could not be explained by the repeatability of the ICP analyses. They[36] considered the possibility of precipitation of different equilibrium phase than Al_8Mn_5 in this region as the most likely cause for the deviations from their solubility model. Their observation together with the results of Nelson[32] and Simensen *et al.*[34,35] suggest that the equilibrium phase in this high temperature and low aluminum concentration region is probably the Beta (CUB) phase. This agrees with the current calculation in this region as shown in Fig. 19. Further, the error bar in this figure indicates that the current calculation is within the error limits of Thorvaldsen's *et al.*[36] measurements.

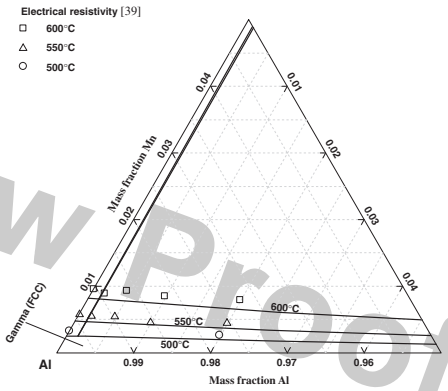

Fig. 20 Calculated solubilities of Mn and Mg in Gamma (FCC) phase compared with the experimental data of Ref. 39).

The calculated solubilities of Mn and Mg in solid Gamma (FCC) phase at different temperatures are compared with the available experimental measurements of Fahrenhorst and Hoffman[39] in Fig. 20 which also shows reasonable agreement with the experimental data.

5. Conclusion

All the experimental phase equilibria and thermodynamic data for the Al-Mn, Mg-Mn and Mg-Al-Mn systems have been collected and evaluated in terms of their reliablity. The current model of the Mg-Mn, Al-Mn and the Mg-Al-Mn systems has extensively been verified by the representative experimental information. In most of the cases, all the current calculations have been found consistent with the experimental observations. Some discrepancies with a few of the experimental data in the Mg-Al-Mn system have been observed. However, the deviations of the current calculations from the experimental information are found acceptable considering the uncertainties of the experiments such as the experimental error limits, probable sample contamination or other experimental conditions. In the absence of exper-

imental data, significant contradictions were found in the calculations of the other existing models predicting the critical temperature of the liquid miscibility gap in the Mg-Mn system. The calculated critical temperature of the liquid miscibility gap with the current model is found consistent with the estimated value using the available empirical equation. In addition to this, some thermodynamic quantities in the Mg-Mn system are compared with other similar systems and found reasonably comparable. Further, A comparison between the current work and the most recent work on the Al-Mn system that uses the same model for the liquid phase reveals that better agreement with the experimental data with less number of model parameters has been achieved in the current work. Above all, the current thermodynamic model of the Mg-Al-Mn system can represent all the reliable experimental phase equilibria and thermodynamic data in a self-consistent manner.

Acknowledgment

The financial support from NSERC (Natural Sciences and Engineering Research Council of Canada) in carrying out this study is gratefully acknowledged.

REFERENCES

1) A. Pelton, S. Degterov, G. Eriksson, C. Robelin and Y. Dessureault: Metall. Mater. **31B** (2000) 651–659.
2) M. Aljarrah: Ph.D. Thesis, Concordia University, (Montreal, Quebec, Canada, 2008).
3) M. Aljarrah and M. Medraj: J. Chem. Thermodyn. **40** (2008) 724–734.
4) M. Aljarrah and M. Medraj: CALPHAD **32** (2008) 240–251.
5) A. Shukla, Y. Kang and A. Pelton: CALPHAD **32** (2008) 470–477.
6) Y. Kang, A. Pelton, P. Chartrand and C. Fuerst: CALPHAD **32** (2008) 413–422.
7) M. Mezbahul-Islam, D. Kevorkov and M. Medraj: J. Chem. Thermodyn. **40** (2008) 1064–1076.
8) A. McAlister and J. Murray: Bull. Alloy Phase Diag. **8** (1987) 438–447.
9) A. Jansson: Metall. Trans. A **23** (1991) 2953–2962.
10) X. Liu, R. Kainuma, H. Ohtani and K. Ishida: J. Alloy. Compd. **235** (1996) 256–261.
11) X. Liu, R. Kainuma and K. Ishida: J. Phase Equilib. **20** (1999) 45–56.
12) C. Müller, H. Stadelmaier, B. Reinsch and G. Petzow: Z. Metallkd. **87** (1996) 594–597.
13) H. Okamoto: J. Phase Equilib. **18** (1997) 398–399.
14) G. Kuznetsov, A. Barsukov and M. Abas: Tsvetn. Met. **1** (1983) 96–100.
15) Y. Minamino, Y. Toshimi, H. Araki, N. Takeuchi, Y. Kang, Y. Miyamoto and T. Okamoto: Metall. Mater. **22A** (1991) 783–786.
16) K. Ishida: CALPHAD **20** (1996) 1–35.
17) A. Livanov and M. Vozdvizhenskii: Trudy Moskov. Avaiatsn. **31** (1958) 65–83.
18) Y. Du, J. Wang, J. Zhao, J. Schuster, F. Weitzer, R. Schmid-Fetzer, M. Ohno, H. Xu, Z. Liu, S. Shang and W. Zhang: Int. J. Mat. Res. **98** (2007) 855–871.
19) A. Shukla and A. Pelton: J. Phase Equilib. Diffus. **30** (2008) 28–39.
20) Y. Esin, N. Bobrov, M. Petrushevski and P. Geld: Zh. Fiz. Khim. **47** (1973) 1959–1962.
21) G. Batalin, E. Beloboradova, B. Stukalo and A. Chekhovskii: Ukr. Khim. Zh. **38** (1972) 825–827.
22) R. Chastel, M. Saito and C. Bergman: J. Alloy. Compd. **205** (1994) 39–43.
23) O. Kubaschewski and G. Heymer: Trans. Farad. Soc. **56** (1960) 473–478.
24) S. Meschel and O. Kleppa: NATO ASI Ser. E **256** (1994) 103–112.
25) R. Kematick and C. Myers: J. Alloy. Compd. **178** (1992) 343–349.
26) A. Hashemi and J. Clark: Bull. Alloy Phase Diag. **6** (1985) 160–164.
27) J. Gröbner, D. Mirkovic, M. Ohno and R. Schmid-Fetzer: J. Phase Equilib. Diffus. **26** (2005) 234–239.
28) Y. Kang, A. Pelton, P. Chartrand, P. Spencer and C. Fuerst: J. Phase Equilib. Diffus. **28** (2007) 342–354.
29) C. Antion: Ph.D. Thesis, Institut National Polytechnique of Grenoble, (2003).
30) M. Ohno and R. Schmid-Fetzer: Z. Metallkd. **96** (2005) 857–869.
31) N. Ageev, I. Kornilov and A. Khlapova: Izvest. Sektora Fiz.-Khim. Anal. **16** (1948) 130–143.
32) B. Nelson: J. Met. **3** (1951) 797–799.
33) M. Mirgalovskaya, L. Matkova and E. Komova: Trudy Inst. Met. **2** (1957) 139–148.
34) C. Simensen, B. Oberlaender, J. Svalestuen and A. Thorvaldsen: Z. Metallkd. **79** (1988) 696–699.
35) C. Simensen, B. Oberlaender, J. Svalestuen and A. Thorvaldsen: Z. Metallkd. **79** (1988) 537–540.
36) A. Thorvaldsen and C. Aliravci: Proc. Int. Symp. on Adv. Prod. Light Met. Met. Matrix Comp. (1992) pp 277–287.
37) W. Leemann and H. Hanemann: Aluminium-Arch **9** (1940) 9–10.
38) W. Hofmann and R. Ovrddot: Aluminium **20** (1938) 865–872.
39) E. Fahrenhorst and W. Hofmann: Metallwissenschaft **19** (1940) 891–893.
40) E. Butchers, G. Raynor and W. Hume-Rothery: J. Ins. Met. **69** (1943) 209–228.
41) A. Little, G. Raynor and W. Hume-Rothery: J. Ins. Met. **69** (1943) 423–440.
42) D. Wakeman and G. Raynor: J. Ins. Met. **75** (1948) 131–150.
43) T. Ohnishi, Y. Nakatani and K. Shimizu: Keikinzoku **23** (1973) 437–443.
44) T. Ohnishi, Y. Nakatani and K. Shimizu: Keikinzoku **23** (1973) 202–209.
45) J. Barlock and L. Mondolfo: Z. Metallkd. **66** (1975) 605–611.
46) H. Fun, H. Lin, T. Jen and B. Yip: Acta Crystallogr. C **50** (1994) 661–663.
47) A. Beerwald: Metallwissenschaft Metalltecknik **23** (1944) 404–407.
48) C. Bale, A. Pelton and W. Thompson: http://www.crct.polymtl.ca (2008).
49) A. Dinsdale: Calphad **15** (1991) 317–425 (updated 2004 version).
50) J. Daams, P. Villars and J. Vucht ed.: *Atlas of Crystal Structure Types for Intermetallic Phases*, (ASM international, Materials Park, Oh:, 1991).
51) A. Westgren: Z. Metallkd. **22** (1930) 368–374.
52) H. Kono: J. Phys. Soc. Jpn. **13** (1958) 1444–1451.
53) E. Butchers and W. Hume-Rothery: J. Ins. Met. **71** (1945) 87–91.
54) M. Drits, E. Kadaner, E. Padezhnova and N. Bochvar: Zh. Neorg. Khim. **9** (1964) 1397–1402.
55) E. Dix, W. Fink and L. Willey: Trans. Am. Inst. Mining Met. Eng. **104** (1933) 335–352.
56) I. Obinata, K. Yamaji and E. Hata: Nippon Kinzoku Gakkaishi **17** (1953) 496–501.
57) T. Goedecke and W. Köster: Z. Metallkd. **62** (1971) 727–732.
58) W. Köster and E. Wachtel: Z. Metallkd. **51** (1960) 271–280.
59) A. Koch, P. Hokkeling, M. Steeg and K. Vos: J. Appl. Phys. **31** (1960) 75–77.
60) J. Murray, A. McAlister, R. Schaefer, L. Bendersky, F. Biancaniello and D. Moffat: Metall. Trans. **18A** (1987) 385–392.
61) M. Drits, Z. Sviderskaya and L. Rokhlin: Issled. Metal. V. Zhidkom I. Tverd. Sostoyaniyakh (1964) 272–278.
62) D. Petrov, M. Mirgalovskaya, I. Strelnikova and E. Komova: Trans. Inst. Met. **1** (1958) 142–143.
63) E. Schmid and G. Siebel: Metallwirtschaft **10** (1931) 923–925.
64) J. Grogan and J. Haughton: J. Inst. Met. **69** (1943) 241–248.
65) M. Chukhov: Inst. Met. A. A. Baikova **1** (1958) 302–305.
66) A. Schneider and H. Stobbe-Scholder: Metall. **4** (1950) 178–183.
67) G. Siebel: Z. Metallkd. **39** (1948) 22–27.
68) N. Tiner: Trans. Met. Soc. AIME **161** (1945) 351–359.
69) B. Predel: Z. Metallkd. **56** (1965) 791–798.
70) R. Singh and F. Sommer: Rep. Prog. Phys. **60** (1997) 57–150.
71) R. Schaefer, F. Biancaniello and W. Cahn: Scr. Metall. **20** (1986) 1439–1444.